Single-wall carbon nanotubes: spintronics in the Luttinger liquid phase

Balázs Dóra[*,1], **Miklós Gulácsi**[1], **Ádám Rusznyák**[2], **János Koltai**[2], **Viktor Zólyomi**[3,4], **Jenö Kürti**[2], **and Ferenc Simon**[5]

[1] Max-Planck-Institut für Physik Komplexer Systeme, Nöthnitzer Str. 38, 01187 Dresden, Germany
[2] Department of Biological Physics, Eötvös University, Pázmány Péter sétány 1/A, 1117 Budapest, Hungary
[3] Department of Physics, Lancaster University, Lancaster, LA1 4YB, UK
[4] Research Institute for Solid State Physics and Optics of the Hungarian Academy of Sciences, Konkoly-Thege M. út 29-33, 1121 Budapest, Hungary
[5] Budapest University of Technology and Economics, Institute of Physics and Solids in Magnetic Fields Research Group, Hungarian Academy of Sciences, P.O. Box 91, 1521 Budapest, Hungary

[*] Corresponding author: e-mail dora@pks.mpg.de, Phone: +49 351 871-2417, Fax: +49 351 871-1999

We study the electron spin resonance (ESR) intensity in the Luttinger liquid phase of carbon nanotubes. The ESR measurables such as the signal intensity and the line-width are calculated in the framework of Luttinger liquid theory with broken spin rotational symmetry as a function of magnetic field and temperature. The linewidth is broadened significantly at high temperatures, and the intensity is well describes by Lorentzians. At very low temperatures, however, the ESR lineshape becomes asymmetric around the resonance, and is characterized by threshold behavior. These observables are of special importance for the spintronics applications of carbon nanotubes.

1 Introduction The effect of electron–electron interaction is an intensively investigated subject of condensed matter physics. Low dimensionality tends to further enhance the importance of correlation, driving the systems into peculiar low temperatures phases. One-dimensional interacting electrons usually form a strange metallic phase, known as Luttinger liquid. In such a state of matter, the fermionic quasiparticle picture breaks down, and the low energy excitations are characterized by a set of bosonic collective density modes (phonons) of the system, which are the true elementary low-energy excitations. A rather faithful realization of this phase is expected to occur in carbon nanotubes, which is confirmed by both the theoretical [1–5] and experimental [6–9] side. In general, low-dimensional carbonaceous systems, fullerenes, carbon nanotubes, and graphene exhibit a rich variety of such phenomena including superconductivity in alkali doped fullerenes [10], quantized transport in single-wall carbon nanotubes (SWCNTs), and massless Dirac quasi-particles showing a half integer quantum hall-effect in graphene even at room temperature [11].

Due to the enhanced effect of correlations in low-dimensional SWCNTs, the physical observables are expected to deviate significantly from those in a conventional Fermi liquid phase. The applicability of SWCNTs for spintronics can only be decided after a careful analysis of their spin relaxation properties. Extensive research in this field is motivated by the orders of magnitude longer conservation of the electron spin alignment in metals as compared to their momentum conservation time [12]. An ideal tool to study the spin relaxation properties of metals is the electron spin resonance (ESR) technique. The spin degeneracy of the energy levels is broken by the application of magnetic field. In the presence of an additional small transversal microwave magnetic field, resonant absorption is induced between the split levels. By changing the value of the longitudinal magnetic field, one determines the position and broadening of the resonance, thus leading to the spin lifetime (the inverse of the linewidth) and g-factor (the position of the resonance). In three-dimensional metals, the ESR signal intensity is proportional to the Pauli spin-susceptibility, the ESR line-width and g-factor are

Phys. Status Solidi B **246**, No. 11–12 (2009)

2745

Original

Paper

determined by the mixing of spin up and down states due to spin-orbit (SO) coupling in the conduction band. These ESR measurables are affected when correlations are present and thus their study holds information about the nature of the correlated state.

This motivated a decade long quest to find the ESR signal of itinerant electrons in SWCNTs and to characterize its properties in the framework of the expected correlations [13–16]. However, to our knowledge no conclusive evidence for this observation has been reported. Let us summarize briefly the current experimental situation: doped SWCNT does not belong to the Luttinger liquid (LL) universality class, but rather forms a Fermi liquid. In this case, the properties of the ESR signal is well documented [14]. In undoped SWCNT, which forms an LL according to photoemission spectroscopy [8, 9], the picture is less clear, and the observation of various signals ranging from Pauli through Curie to super-Curie explains the debate on the inherent signal of LL. An often cited argument for this anomalous absence of the ESR signal is the large heterogeneity of the system, the lack of crystallinity, and the presence of magnetic catalyst particles [13–16]. However, this would also prevent the observation of the ESR signal of doped SWCNTs [14]. Thus the above properties of SWCNTs should hinder the observation of the ESR signal also for the Fermi liquid state, which is clearly not the case. We suggest that the LL state inherently prohibits the observation of ESR of the itinerant electrons, calling for a realistic description of such experiments. A recent experiment by Kuemmeth et al. [17] shed new light on the spin degree of freedom of SWCNTs. It was shown that SO coupling and correspondingly the lifting of the spin rotational invariance is unexpectedly large. As we show below, this results in a uniquely large homogeneous broadening of the ESR line which explains the absence of an intrinsic ESR signal of SWCNTs. Previous theories of ESR in the SWCNTs concentrated on non-interacting spin sector with SO coupled quasiparticles [18, 19].

One-dimensional interacting fermions usually form a Luttinger liquid, which replaces the canonical Fermi liquid picture in higher dimensions. The quasiparticle description breaks down and low energy properties are described by critical phenomena of collective modes for this state of the matter due to restricted dimensionality and interactions [20, 21]. This results in anomalous power-law dependence of correlation functions at low energies, with critical exponents changing continuously with the interaction strength. Another hallmark of LL is spin-charge separation, spin and charge excitations propagate with different velocities due to the complicated many body ground state, caused by the interactions.

Here, we study the ESR signal in an LL with broken spin rotational symmetry. While at low temperatures the characteristic non-integer power laws characterize the response, the high temperature behavior crosses over to the standard Lorentzians, whose width, in contrast to the Fermi liquid picture [22], is determined by the LL parameters. We show that this explains the absence of itinerant ESR in this system by combining DFT calculations of the spin-susceptibility on metallic SWCNTs with a critical evaluation of the experimental conditions.

To describe a metallic SWCNT, we apply an effective low-energy theory. We neglect the "flavour" index coming from the two K points [19] since we are interested in the spin properties only. The standard LL Hamiltonian is expressed as a sum of independent spin and charge excitations as

$$H = \sum_{\nu=c,s} \frac{\hbar v_\nu}{2} \int dx \left(K_\nu \Pi_\nu^2 + \frac{1}{K_\nu} (\partial_x \phi_\nu)^2 \right), \quad (1)$$

where K_ν are the LL parameters, $\nu = c, s$ denotes the charge and spin sector, respectively, Π_ν and ϕ_ν are canonically conjugate fields with velocity v_ν. The LL parameter in the spin sector, $K_s = 1$ for SU(2) symmetric models as these preserve the spin rotational symmetry. However, the presence of SO and magnetic dipole–dipole interaction between the conduction electrons [20, 23] produces spin dependent interactions and breaks the spin rotational symmetry, leading to $K_s \neq 1$. In addition, these processes are also responsible for the g-factor anisotropy. The motion of the electrons is restricted in the x direction.

The original fermionic field operators are expressed in terms of the bosons as

$$\Psi_{r\sigma}(x) = \frac{\eta_{r\sigma}}{\sqrt{2\pi\alpha}} \times$$
$$\times \exp\left(i\sqrt{\frac{\pi}{2}} (r\phi_c(x) + r\sigma\phi_s(x) + \Theta_c(x) + \sigma\Theta_s(x)) \right), \quad (2)$$

which are needed to express the spin operators in the bosonic language, $\eta_{r\sigma}$ is the Klein factor, $\Theta_\nu(x) = -\int_{-\infty}^{x} dx' \Pi_\nu(x')$, $r = R/L = \pm$ denotes the chirality of the electrons, and $\sigma = \pm$ is the electron spin.

The ESR experiments are performed in a longitudinal static magnetic field, B, applying a transversal perturbing microwave radiation with a magnetic component, $B_\perp$. For the ESR description, the above Hamiltonian is completed with the Zeeman term:

$$H_Z = -g\mu_B B \int dx \partial_x \phi_s(x). \quad (3)$$

The ESR signal intensity is given by the absorbed microwave power that is [22]:

$$I(\omega) = \frac{B_\perp^2 \omega}{2\mu_0} \chi''_\perp(q = 0, \omega) V, \quad (4)$$

where μ_0 is the permeability of the vacuum, $\chi''_\perp$ the imaginary part of the retarded spin-susceptibility for the transversal direction, and V is the sample volume. The spin operators required to calculate $\chi''_\perp$ are

$$S^\pm(x) = \sum_{r,r'} \exp(i(r' - r)k_F) \Psi_{r\pm}^+(x) \Psi_{r'\mp}(x). \quad (5)$$

Since ESR measures the $q = 0$ response, only the $r = r'$ terms contribute, the others contain fast oscillating terms $\sim \exp(\pm 2ik_F)$ and average to zero.

The Zeeman term in Abelian bosonization is the simplest when the longitudinal magnetic field points in the spin quantization axis (the z-axis). For a different field orientation, the Zeeman term becomes more complicated but it can be rotated along the z direction, at the expense of changing the LL parameters K_ν [23]. The external magnetic field further lowers the SU(2) symmetry in addition to the SO and dipole–dipole interactions, resulting in a further renormalization of K_s.

From now on, we set $\hbar = k_B = g\mu_B = 1$ and they will be reinserted whenever necessary. The retarded spin-susceptibility is built up from correlators of the type [24]

$$\langle S^+(x,t)S^-(0,0)\rangle = c_\perp^2 \left(\frac{\pi T \alpha / v_s}{\sin h[\pi T(x/v_s - t + i\alpha)]} \right)^{2+\gamma}$$
$$\times \left(\frac{\pi T \alpha / v_s}{\sin h[\pi T(x/v_s + t - i\alpha)]} \right)^\gamma \exp\left(\frac{ibx}{v_s} \right),$$
(6)

where $b = K_s B$, $c_\perp$ is determined by the short distance behavior and cannot be obtained by the methods used here. Here we introduced the $\gamma = (K_s + 1/K_s - 2)/2$ parameter, which encodes information about spin symmetry breaking processes. Upon Fourier transformation, we obtain the retarded spin-susceptibility. From a simple scaling analysis, we can conjecture the behavior of the retarded spin-susceptibility as

$$\chi(q = 0, \omega)_\perp \sim \max[B, \omega, T]^{2\gamma},$$
(7)

which is confirmed below.

Putting all this together, we find for the ESR intensity (following Ref. [21], Appendix C):

$$I(\omega) = -A \sin(\pi\gamma)\omega \left(\frac{2\pi\alpha T}{v_s} \right)^{2\gamma}$$
$$\times \text{Im}[F(2+\gamma, k_+)F(\gamma, k_-)F(2+\gamma, k_-)F(\gamma, k_+)],$$
(8)

where

$$k_\pm = \frac{\omega \mp b}{2\pi T},$$
(9)

$$F(x,y) = B\left(\frac{x - iy}{2}, 1 - x \right),$$
(10)

where $B(x,y) = \Gamma(x)\Gamma(y)/\Gamma(x+y)$ is Euler's beta function, $\Gamma(x)$ is Euler's gamma function, A is a constant, whose value is determined further below. In the $\gamma = 0$ limit, SU(2) spin symmetry is conserved by the Hamiltonian and the ESR resonance becomes completely sharp, located at $\pm B$ as $\sim B^2\delta(\omega \pm B)$.

The influence of interactions is most clearly seen at $T = 0$, when the ESR signal is completely asymmetric around $\omega = \pm b$, and cannot be approximated by Lorentzians:

$$I(\omega) = A\left(\frac{\alpha}{2v_s} \right)^{2\gamma} \sin^2(\pi\gamma) \frac{\Gamma^2(1-\gamma)}{\gamma(1+\gamma)}$$
$$\times \frac{2|\omega|(\omega^2 + b^2)}{(\omega^2 - b^2)^{1-\gamma}},$$
(11)

for $|\omega| > b$, and zero otherwise. The ESR intensity vanishes below a threshold set by the magnetic field, and falls off in a power law fashion, depending on the explicit value of K_s, and is shown in Fig. 1.

However, the sharp threshold disappears with increasing temperature and the spectrum broadens. In the limit of $T \gg \omega$, B and $\gamma \ll 1$, which is relevant for realistic experiments, the intensity can be approximated by (upon reinserting original units)

$$I(\omega) = A2\pi(\hbar\omega)^2$$
$$\times \left[\frac{\eta}{(\hbar\omega - K_s g\mu_B B)^2 + \eta^2} + \frac{\eta}{(\hbar\omega + K_s g\mu_B B)^2 + \eta^2} \right],$$
(12)

where

$$\eta = 2\gamma\pi k_B T.$$
(13)

This expression works well outside of its range of validity and it consists of two Lorentzians, centered around $\pm K_s g\mu_B B$, characterized by a width of η. Hence, the interaction (γ) together with the temperature determines
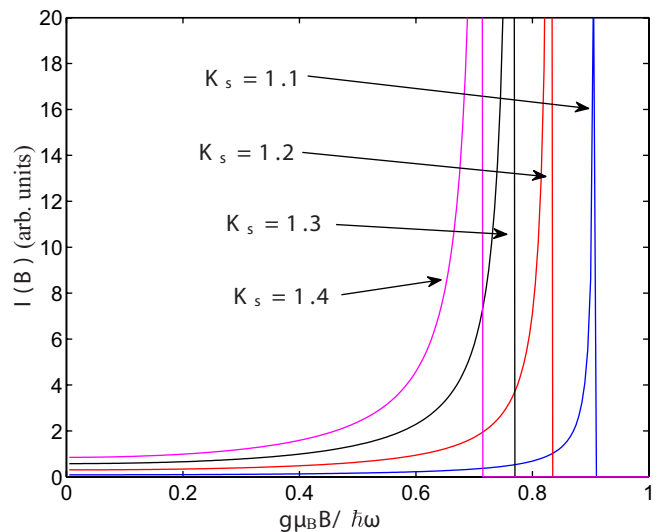

Figure 1 (online colour at: www.pss-b.com) The ESR *signal* intensity, Eq. (11) is shown at $T = 0$ as function of the magnetic field for $K_s = 1.1$, 1.2, 1.3, and 1.4. The resonance occurs at $g\mu_B B/\hbar\omega = 1/K_s$. The asymmetric intensity reflects the LL nature of the ground state.
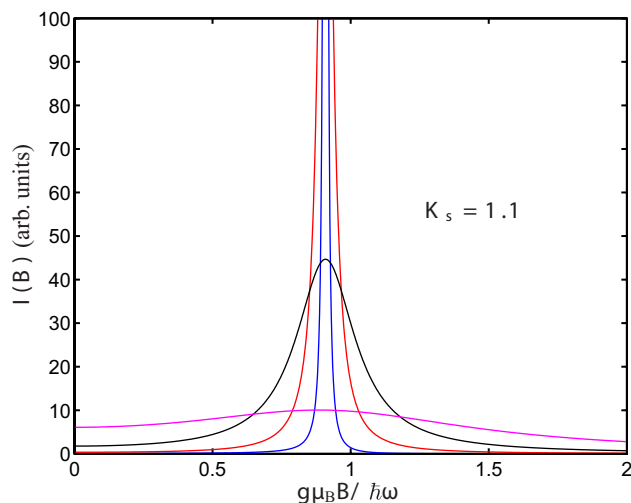
Phys. Status Solidi B **246**, No. 11–12 (2009)

2747

Original

Paper

Figure 2 (online colour at: www.pss-b.com) The ESR *signal* intensity, Eq. (8) is shown as a function of the magnetic field for $K_s = 1.1$ (corresponding to $\gamma = 0.0045$), $k_B T/\hbar\omega = 0.1$ (blue), 1 (red), 5 (black), and 25 (magenta). The resonance occurs at $g\mu_B B/\hbar\omega = 1/K_s \approx 0.91$ for small temperatures.
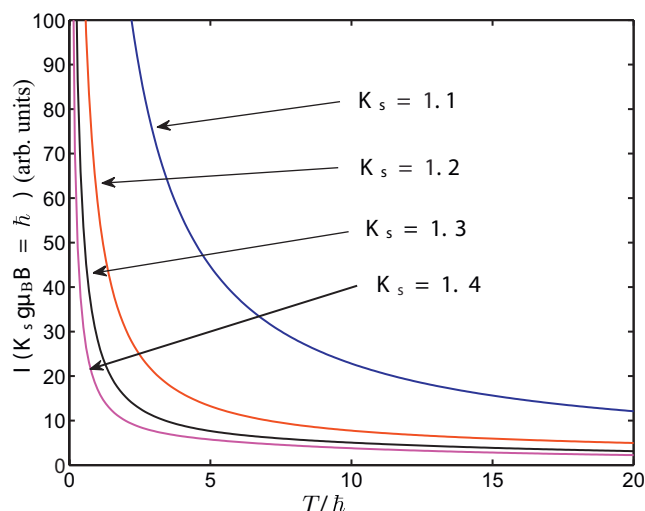

Figure 4 (online colour at: www.pss-b.com) The resonance peak in the ESR *signal* intensity is shown as a function of temperature for for $K_s = 1.1$, 1.2, 1.3, and 1.4. The resonance occurs at $g\mu_B B/\hbar\omega = 1/K_s$.

the width of the resonance and shifts the resonance center as well, as is seen in Figs. 2 and 3 for $K_s = 1.1$ and 1.3, respectively. In Fig. 4, the evolution of the resonance peak with temperature is shown for various K_s.

This expression allows us to make contact with the conventional Fermi liquid case. In that case, $K_s = 1$ (together with $\gamma \to 0$), which signals a non-interacting spin sector. The ESR intensity reduces to

$$I(\omega) = A2\pi^2(g\mu_B B)^2[\delta(\hbar\omega - g\mu_B B) + \delta(\hbar\omega + g\mu_B B)]. \tag{14}$$
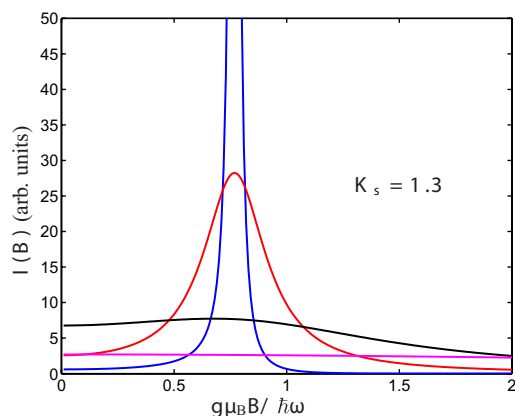

Figure 3 (online colour at: www.pss-b.com) The ESR *signal* intensity, Eq. (8) is shown as a function of the magnetic field for $K_s = 1.3$ (corresponding to $\gamma = 0.0045$), $k_B T/\hbar\omega = 0.1$ (blue), 1 (red), 5 (black), and 25 (magenta). The resonance occurs at $g\mu_B B/\hbar\omega = 1/K_s \approx 0.77$ for small temperatures.

Thus the integrated ESR intensity reads as $\int d\omega I(\omega)/\omega = A4\pi^2 g\mu_B B$. In a Fermi liquid, this is expressed in terms of the static spin-susceptibility [22], χ_0, as $\int d\omega I(\omega)/\omega = \chi_0 B_\perp^2 V\pi g\mu_B B/2\mu_0\hbar$. This fixes the so far unknown numerical prefactor as $A = \chi_0 B_\perp^2 V/2\mu_0\hbar\pi$. In summary, the ESR signal of an LL with broken spin rotational symmetry (i) is significantly broadened due to the interaction and spin symmetry breaking and (ii) has a signal intensity which matches that of the non-interacting state.

These results are similar to those found for the 1D antiferromagnetic Heisenberg model [25], whose low energy theory is identical to the spin sector of a Luttinger liquid, Eq. (1). The ESR line-width also scales with T at low temperatures. However, the spin in the Heisenberg model, when represented in terms of fermionic variables via the Jordan–Wigner transformation, usually contains non-local string operators [21] and acquires a different scaling dimension than the spin of itinerant electrons. The exchange anisotropy, causing the broadening of the ESR signal, shares common origin with the g-factor anisotropy in terms of SO coupling, scaling with $(\Delta g/g)^2$.

In Refs. [18, 19], a non-interacting spin sector was considered (with $K_s = 1$) together with explicitly SO coupled quasiparticles, leading to a narrow two peak spectrum. Our approach takes general spin anisotropies due to SO coupling, spin backscattering, dipole-dipole interactions and magnetic field into account in our starting Hamiltonian [Eq. (1)]. These processes introduce interactions in the spin sector [23], resulting in $K_s \neq 1$.

The SO coupling in SWCNTs was found to be unexpectedly large, around 1 meV for a nanotube with diameter of 1 nm, resulting in a g-factor enhancement

$g = 2.14$ in a few electron carbon nanotube quantum dot [17]. According to our theory, the position of the resonance occurs at $K_s g$ with the bare g-factor, which leads us to $K_s \sim 1.07$. In addition, $K_s \sim 1.3$ for quantum wires [26] like InAs, which is another possible realization of LL. These materials possess a SO coupling of the same order of magnitude than SWCNTs but they have a three times smaller Fermi velocity. Following a similar line of reasoning for SWCNTs, we use [21] $K_s \approx 1 + g_s/(2\pi v_F)$ with g_s the effective interaction in the spin sector using the g-ology notations [19, 21], influenced by the SO coupling (the same as for quantum wires [26], but with $v_F \approx 3v_{F,wire}$). Based on all this, we take a conservative estimate of K_s to be around 1.1.

In the following, we discuss the relevance of the results on the absence of an ESR signal in SWCNTs. As we showed above, the ESR signal intensity of an LL crosses over smoothly for the non-correlated case to the static susceptibility that is the Pauli susceptibility of metallic SWCNTs [27]: $\chi_0 = \mu_0 g^2 \mu_B^2 D(E_F)/4$, where $D(\varepsilon_F)$ is the density of states (DOS) at the Fermi energy. To have an accurate value for the DOS in a realistic sample, we performed density functional theory calculations with the Vienna *ab initio* Simulation Package [28] within the local density approximation for metallic nanotubes. The projector augmented-wave method was used with a plane-wave cutoff energy of 400 eV. The DOS was obtained with a Green's function approach from the band structure. We considered the SWCNTs with chiral indices (9,9), (15,6), (10,10), (18,0), and (11,11) [29]. These tubes are within the Gaussian diameter distribution of a usual SWCNT sample with a mean diameter of 1.4 nm and a variance of 0.1 nm. We confirmed by nearest-neighbor tight binding calculations on all the metallic SWCNTs in the above diameter distribution that the DOS depends very weakly on the chirality, thus the above SWCNTs chiralities are indeed representative for the ensemble of the metallic tubes.

We obtain that such a tube ensemble has a DOS of $D(E_F) = 4.6 \times 10^{-3}$ states/eV/atom by averaging the DOS for the above SWCNTs and taking into account that only one third of the tubes are metallic for this diameter range [29]. This is a very low DOS which results from the one-dimensionality of the tubes and from the fact that the majority of the tubes are non-metallic. It is 50 times smaller than in K_3C_{60} [$D(E_F) \approx 0.3$ states/eV/atom [10]] and is comparable to the low DOS of pristine graphite [$D(E_F) \approx 5 \times 10^{-3}$ states/eV/atom [30]]. With the above DOS, we obtain that a typical 2 mg SWCNT sample gives a practically detectable signal-to-noise ratio of $S/N = 10$ for a spectrum measured for 1000 s provided the ESR line is not broader than 110 mT. To obtain this value, we considered that the state-of-the-art ESR spectrometers give an $S/N = 1$ for 10^{10} $S = 1/2$ spins at 300 K provided the ESR line-width is 0.1 mT and each spectra points (typically 1000) are measured for 1 s. We also took into account that the S/N drops with the square of the line-width for broadening beyond 1 mT.

The above calculated homogeneous broadening of the ESR line of an LL is $2\pi\gamma k_B T/g\mu_B$ in units of the magnetic field. Thus at 4 K, which is the lowest available temperature for most ESR spectrometers, one has a broadening of γ 18.7 Tesla. This, together with the above detectability criterion gives an upper limit of $\gamma = 6 \times 10^{-3}$ for the detection of the ESR signal. Clearly, the above conservative estimate of $\gamma = 4.5 \times 10^{-3}$ based on the $K_s = 1.1$ value is close to this limit, which explains why careful studies have not yet yielded a conclusive ESR signal of itinerant electrons is SWCNTs. This argument might also be turned around: the fact that no ESR signal of the itinerant electron has been observed in the SWCNTs means that the line is broadened beyond observability, which is translated to $\gamma > 6 \times 10^{-3}$, putting also $K_s > 1.1$. However, other factors, such as, *e.g.*, limited microwave penetration into the SWCNT sample further limits ESR experiments, leading to the unobservability of ESR for smaller values of γ and K_s as well.

We finally comment on the future viability of this observation. Clearly, ESR spectrometers operating to sub Kelvin temperatures are required. Observation of linearly temperature dependent ESR line-width would be an unambiguous evidence for the observation of the ESR signal of itinerant electrons in the LL state. Such a temperature dependence is fairly unusual as ESR line-width in metals normally tends to a residual value similar to the resistivity.

In summary, we extended the theory of ESR in an LL for the case of broken spin-symmetry with interacting spin sector. We obtain a significant homogeneous broadening of the ESR line-width with increasing temperature, which explains the unobservability of ESR in SWCNTs and puts severe constraints on the usability of SWCNTs for spintronics.

References

[1] R. Egger and A. O. Gogolin, Eur. Phys. J. B **3**, 281–300 (1998).

[2] C. Kane, L. Balents, and M. P. A. Fisher, Phys. Rev. Lett. **79**, 5086–5089 (1997).

[3] L. Balents and M. P. A. Fisher, Phys. Rev. B **55**, R11973–R11976 (1997).

[4] H. Yoshioka and A. A. Odintsov, Phys. Rev. Lett. **82**, 374 (1999).

[5] Y. A. Krotov, D. H. Lee, and S. G. Louie, Phys. Rev. Lett. **78**, 4245–4248 (1997).

[6] M. Bockrath, D. H. Cobden, J. Lu, A. G. Rinzler, R. E. Smalley, L. Balents, and P. L. McEuen, Nature **397**, 598–601 (1999).

[7] B. Gao, A. Komnik, R. Egger, D. C. Glattli, and A. Bachtold, Phys. Rev. Lett. **92**, 216804–1–4 (2004).

[8] H. Ishii, H. Kataura, H. Shiozawa, H. Yoshioka, H. Otsubo, Y. Takayama, T. Miyahara, S. Suzuki, Y. Achiba, M. Nakatake, T. Narimura, M. Higashiguchi, K. Shimada,

Phys. Status Solidi B **246**, No. 11–12 (2009)

2749

H. Namatame, and M. Taniguchi, Nature **426**, 540 (2003).

[9] H. Rauf, T. Pichler, M. Knupfer, J. Fink, and H. Kataura, Phys. Rev. Lett. **93**, 096805 (2004).

[10] O. Gunnarsson, Rev. Mod. Phys. **69**, 575–606 (1997).

[11] K. S. Novoselov, A. K. Geim, S. V. Morozov, D. Jiang, M. I. Katsnelson, I. V. Grigorieva, S. V. Dubonos, and A. A. Firsov, Nature **438**, 197–200 (2005).

[12] I. Žutić, J. Fabian, and S. D. Sarma, Rev. Mod. Phys. **76**, 323–410 (2004).

[13] P. Petit, E. Jouguelet, J. E. Fischer, A. G. Rinzler, and R. E. Smalley, Phys. Rev. B **56**, 9275–9278 (1997).

[14] A. S. Claye, N. M. Nemes, A. Jánossy, and J. E. Fischer, Phys. Rev. B **62**, 4845–4848 (R) (2000).

[15] J. P. Salvetat, T. Fehér, C. L'Huillier, F. Beuneu, and L. Forró, Phys. Rev. B **72**, 075440–1–6 (2005).

[16] V. Likodimos, S. Glenis, N. Guskos, and C. L. Lin, Phys. Rev. B **76**, 075420 (2007).

[17] F. Kuemmeth, S. Ilani, D. C. Ralph, and L. M. McEuen, Nature **452**, 448 (2008).

[18] A. De Martino, R. Egger, K. Hallberg, and C. A. Balseiro, Phys. Rev. Lett. **88**, 206402 (2002).

[19] A. De Martino, R. Egger, F. Murphy-Armando, and K. Hallberg, J. Phys.: Condens. Matter **16**, S1427 (2004).

[20] A. O. Gogolin, A. A. Nersesyan, and A. M. Tsvelik, Bosonization and Strongly Correlated Systems (Cambridge University Press, Cambridge, 1998).

[21] T. Giamarchi, Quantum Physics in One Dimension (Oxford University Press, Oxford, 2004).

[22] C. P. Slichter, Principles of Magnetic Resonance, 3rd ed. (Spinger-Verlag, New York, 1989).

[23] T. Giamarchi and H. J. Schulz, J. Phys. France **49**, 819 (1988).

[24] H. J. Schulz, Phys. Rev. B **34**, 6372 (1986).

[25] M. Oshikawa and I. Affleck, Phys. Rev. B **65**, 134410 (2002).

[26] V. Gritsev, G. Japaridze, M. Pletyukhov, and D. Baeriswyl, Phys. Rev. Lett. **94**, 137207 (2005).

[27] N. W. Ashcroft and N. D. Mermin, Solid State Physics (Holt Rinehart and Winston, New York 1976).

[28] G. Kresse and J. Furthmüller, Phys. Rev. B **54**, 11169 (1996).

[29] R. Saito, G. Dresselhaus, and M. Dresselhaus, Physical Properties of Carbon Nanotubes (Imperial College Press, London 1998).

[30] M. Dresselhaus and G. Dresselhaus, Adv. Phys. **30**, 139 (1981).